

Bringing Microphysics to the Masses: The Blowing Snow Observations at the University of North Dakota

Education through Research (BLOWN-UNDER) Campaign

Aaron Kennedy, Aaron Scott, Nicole Loeb, Alec Szczepanski, Kaela Lucke,
Jared Marquis, and Sean Waugh

ABSTRACT: Harsh winters and hazards such as blizzards are synonymous with the northern Great Plains of the United States. Studying these events is difficult; the juxtaposition of cold temperatures and high winds makes microphysical observations of both blowing and falling snow challenging. Historically, these observations have been provided by costly hydrometeor imagers that have been deployed for field campaigns or at select observation sites. This has slowed the development and validation of microphysics parameterizations and remote sensing retrievals of various properties. If cheaper, more mobile instrumentation can be developed, this progress can be accelerated. Further, lowering price barriers can make deployment of instrumentation feasible for education and outreach purposes. The Blowing Snow Observations at the University of North Dakota: Education through Research (BLOWN-UNDER) Campaign took place during the winter of 2019/20 to investigate strategies for obtaining microphysical measurements in the harsh North Dakota winter. Student led, the project blended education, outreach, and scientific objectives. While a variety of in situ and remote sensing instruments were deployed for the campaign, the most novel aspect of the project was the development and deployment of OSCRE, the Open Snowflake Camera for Research and Education. Images from this instrument were combined with winter weather educational modules to describe properties of snow to the public, K–12 students, and members of indigenous communities through a tribal outreach program. Along with an educational deployment of a Doppler on Wheels mobile radar, nearly 1,000 individuals were reached during the project.

KEYWORDS: North America; Snow; In situ atmospheric observations; Surface observations; Field experiments

<https://doi.org/10.1175/BAMS-D-20-0199.1>

Corresponding author: Aaron Kennedy, aaron.kennedy@und.edu

In final form 14 July 2021

©2022 American Meteorological Society

For information regarding reuse of this content and general copyright information, consult the [AMS Copyright Policy](#).

AFFILIATIONS: Kennedy, Scott, Sczepanski, Lucke, and Marquis—Department of Atmospheric Sciences, University of North Dakota, Grand Forks, North Dakota; Loeb—Department of Environment and Geography, University of Manitoba, Winnipeg, Manitoba, Canada; Waugh—NOAA/National Severe Storms Laboratory, Norman, Oklahoma

Harsh winters and hazards such as blizzards are synonymous with the northern Great Plains of the United States. The earliest records of the challenges these conditions posed on locals come from Plains Indian tribes like the Lakota who recorded their history via pictographs in winter counts (*waniyetu wówapi*) on mediums such as animal hides (Green and Thornton 2007; Therrell and Trotter 2011; Howe 2015). Extending for over 100 years in some cases, these historical records documented events such as significant snowfalls, animal deaths due to cold weather, and floods from ice dam breaks. As westerners settled the region in the 1800s, they too were met with the ferocity of winter with stories such as the winter of 1880/81 (Wilder 1940; Boustead 2014; Boustead et al. 2020), the Children’s Blizzard in 1888 (Laskin 2005), and the sacrifice of Hazel Miner to save her siblings during a blizzard in 1920 (Kremer 2015) permeating regional culture.

Fast forwarding to present day, advancements in science have improved our understanding of blizzards and the underlying processes of falling and blowing snow. From pattern recognition of these events using reanalyses (Kennedy et al. 2019), to satellite and radar-based detection of the hazard (e.g., Palm et al. 2011; Kennedy and Jones 2020), to empirical techniques of predicting blowing snow (Baggaley and Hanesiak 2005; NOAA 2020), a variety of tools now exist to aid forecasters with forecasting winter hazards in this region.

Despite these advancements, forecasting blowing and falling snow is an imperfect science. While blizzards are often thought of as the juxtaposition of wind and significant falling snow, these events can also occur without active precipitation. Coined ground blizzards (Stewart et al. 1995; Kapela et al. 1995), these events can have impressive spatial heterogeneity (Kennedy and Jones 2020), and are dependent on nuances of the land surface and atmosphere including snowpack age, temperature, and wind speed (Li and Pomeroy 1997a,b; Baggaley and Hanesiak 2005). Because significant snowfall is not expected with ground blizzards, they can take individuals by surprise, and stories of stranded travelers are a common news headline in the region during the winter.

Operational models should include parameterizations for blowing snow, but measurements in both time and space are lacking to develop and evaluate such schemes. The cold temperatures and strong winds associated with either type of blizzard make observations challenging. Furthermore, blowing snow events can be difficult to anticipate given sparse observations of the snowpack leading up to these events. Simply measuring snowfall is difficult as noted in winter precipitation testbeds (e.g., Rasmussen et al. 2012), and this poses downstream impacts on blizzard forecasting. Most societal impacts revolve around visibility, with both falling and blowing snow contributing to extinction of light. Given the difficulties in representing this variable through modeling, visibility is an imperfect variable for assessment of event processes and hazards. Instead, direct microphysical measurements are needed and the presence of falling and/or blowing snow requires instrumentation that can measure particles ranging from 10 to 10⁴ μm.

A number of techniques have been developed to measure microphysical properties at the surface. While a full survey is beyond the scope of this article, observations range from manual inspection of particles with microscopes (e.g., Shimizu 1963) or cell phones (Kumjian et al. 2020) to instruments that use visible and near-infrared light to obtain properties such as size, shape, and number concentration. Laser-based instruments including the snow-particle counter (SPC; Schmidt 1977; Sato et al. 1993) and the OTT particle size

velocity disdrometer (Parsivel²; Löffler-Mang and Joss 2000; Tokay et al. 2013; see the appendix for a list of acronyms and definitions) can measure particle size distributions (PSDs), while optical imagers including the 2D video disdrometer (2DVD; Schönhuber et al. 2007), the Snow Video Imager (SVI; Newman et al. 2009), the Precipitation Imaging Package (PIP; Pettersen et al. 2020), and the Multi-Angle Snowflake Camera (MASC; Garrett et al. 2012) provide images that can be used to derive PSDs and determine particle phase/habit. These observations have also been acquired via ground deployment of aircraft optical probes such as the Cloud Particle Imager (CPI; Lawson et al. 2001, 2006). Other devices such as manual snow traps (Mellor and Radok 1960) and the acoustic FlowCapt (Chritin et al. 1999) can observe bulk properties such as mass flux of blowing/drifting snow.

While these instruments have many strengths, several broad weaknesses exist. Microphysical observations are generally expensive compared to other in situ atmospheric measurements. For example, temperature sensors are typically <\$1,000 USD while aircraft probes can cost >\$100,000 USD. This limits deployments to specific sites or for limited field campaigns. While the cost is justified due to the complexity and limited market for these instruments, it poses a barrier that 1) slows science and 2) hampers their widespread use for educational and outreach objectives. Further, many of the current instruments are flawed when it comes to sampling snowfall or blizzard environments. Accurate sizing of a broad range of particles during falling or blowing snow events is an issue for instruments like the Parsivel² (Battaglia et al. 2010; Loeb and Kennedy 2021) while instruments with enclosed sampling volumes like the MASC raise the likelihood of interactions with the environmental wind field (Fitch et al. 2021). Other instruments such as the PIP are not commercially available. In light of these issues, affordable microphysics instrumentation capable of operating in snowfall or blizzard environments needs to be developed and tested. Further, these designs should be of open nature like the SVI or PIP to minimize wind effects.

The Blowing Snow Observations at the University of North Dakota: Education through Research (BLOWN-UNDER) Campaign took place during the winter of 2019/20 to investigate strategies for attaining microphysical measurements in harsh winter environments. This project served as the first real world test for OSCRE, the Open Snowflake Camera for Research and Education. OSCRE was deployed throughout the winter, collecting 93 h of observations across 19 different precipitation and blowing snow events. Recorded events ranged from 0.5 to 12 h of observation time with a mean and standard deviation of 4.9 ± 3.8 h. An intensive operation phase (IOP) of the project was held from 20 January to 13 February 2020 to coincide with an educational deployment of a Center for Severe Weather Research Doppler on Wheels (DOW7). The project also tested the recently upgraded balloon-borne Particle Size and Velocity (PASIV) probe (Vaugh et al. 2015). While the IOP period was generally quiescent, the campaign concluded with a classic ground blizzard on 12 February 2020.

The purpose of this article is to highlight OSCRE and the BLOWN-UNDER campaign. The entwinement of science, education, and outreach objectives of the project are emphasized. Preliminary data from the 12 February 2020 ground blizzard are presented throughout to highlight the success of the campaign. The article concludes with lessons learned from the experience.

Developing OSCRE

OSCRE takes design cues from the PIP and PASIV to create an affordable hydrometeor imaging system for ground deployments. Major components of the system include a USB3 machine vision camera and lens, a computing platform that controls the camera, and a strobed LED light triggered by output from the camera. Collectively, the system is capable of resolving hydrometeors down to $\sim 50 \mu\text{m}$ in diameter. Components are housed within commercially available heated housings and mounted to a simple, treated lumber platform (Fig. 1). A full list

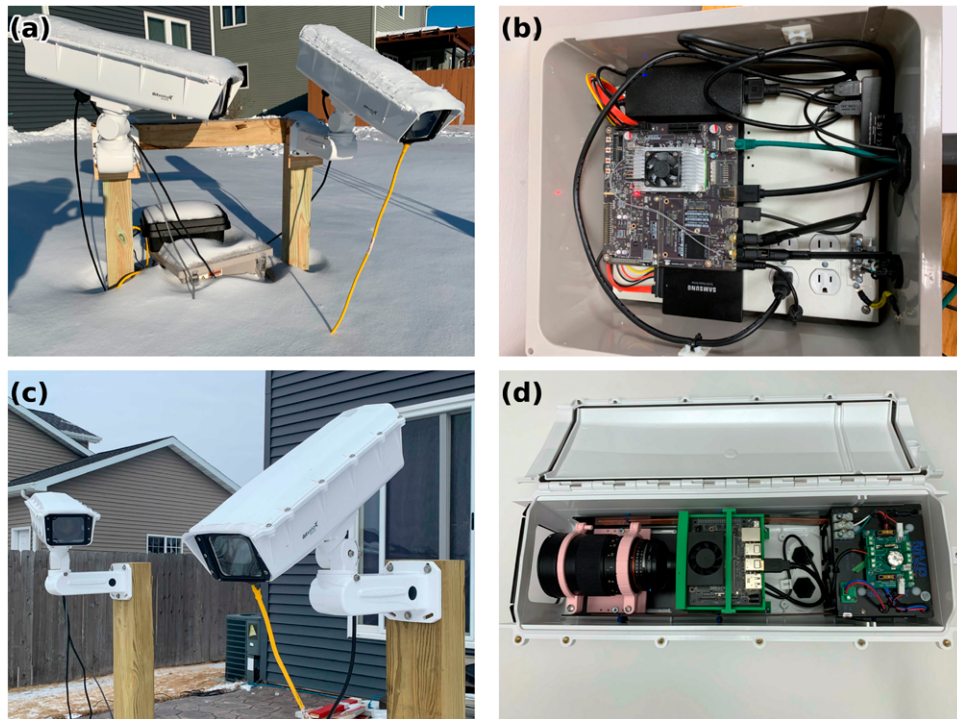


Fig. 1. OSCORE configurations for (a),(b) the winter of 2019/20 and (c),(d) present day. Panels (a) and (c) represent focal lengths of 0.8 and 1.5 m, respectively. Panel (b) shows the original Nvidia Jetson TX2 contained within an externally mounted heated housing. In (d), OSCORE is shown with a Jetson Xavier NX mounted internally within the camera housing using 3D printed brackets.

Table 1. Components and prices for OSCORE. Prices in parentheses represent aftermarket cost.

Component	Details	Approximate price (as of March 2021)
Camera	FLIR Blackfly S (USB3) BFS-U3-04S2C-CS <ul style="list-style-type: none"> • 3.2MP, 1/1.8" sensor (Sony IMX252 CMOS) • 118 fps, global shutter 	\$800
Lens	Rokinon 135 mm F/2 for Nikon F mount <ul style="list-style-type: none"> • Requires Fotodiox Nikon F to C-Mount Adapter • Minimum focus distance: 0.8 m • Manual aperture/focus controls 	\$600
Computer	NVIDIA Xavier NX Developer Kit <ul style="list-style-type: none"> • NVIDIA Volta GPU, 6-core ARM CPU • 8 GB memory 	\$400
Storage	64 GB SanDisk Extreme microSDXC (OS) 2TB Samsung 970 EVO Plus SSD M.2 NVMe (Data)	\$350
Lighting	SmartVisionLights ODS75-WHI OverDrive Brick Light <ul style="list-style-type: none"> • Includes power supply + cabling 	\$500
Housings	2 × Dotworkz ST-RF-MVP housings <ul style="list-style-type: none"> • Heated, require AC cable Significant savings via aftermarket	\$1,300 (\$300)
Cables/Misc	HDMI Dummy Plug 1 ft Micro USB 3.0 Cable. A male to Micro B (up angle) + locking screws CAT6 cable	\$50
Misc.	Lumber for structure, mechanical hardware, 3D printed parts, etc.	\$200
Total		\$4,200 (\$3,200)

of components and approximate prices at time of publication are listed in Table 1. The open design of the instrument, parts lists and instructions are provided at <https://github.com/KennedyClouds/OSCRE>. Details on the imaging system are provided in the sidebar.

Design. Compared to other systems, OSCRE is unique in its use of affordable strobed lighting to “freeze” hydrometeors as they pass through the frame. The system uses a Smart Vision Lights ODS75 brick light with narrow lenses to strobe the sampling volume. A singular light is aimed from the side and slightly forward of the focal plane (Figs. 1a,c). This is adequate to image hydrometeors at an exposure time of 5–10 μ s at a distance of ~20 cm. A major advantage of this light is an internal controller that greatly simplifies the triggering process. The strobe is activated by a pulse generator on the camera or simply when the exposure is occurring. While the system is effective, strobing at visible wavelengths can cause issues with individuals with light sensitivity.

Weatherproofing is a challenge for any instrument. To handle harsh winter conditions, OSCRE uses two, IP66 rated dotworkz ST-RF-MVP camera housings. These units include 65 W internal heaters with a blower unit supporting temperatures down to -60°F . While temperatures to this extreme were not observed during BLOWN-UNDER, the system had no issues handling conditions down to -20°F , and no downtime was caused due to weather. An additional benefit of these housings is included 12/24 V output adequate to power the camera and computer (<20 W). A separate power supply is needed for the lighting due to the draw needed during individual strobes.

The final complexity of developing instrumentation is connectivity of equipment. To avoid the expenses with machining, the current generation of OSCRE relies on 3D printed parts created with OpenSCAD (Fig. 1d). The project uses an open hardware lens mount modified with a base plate to attach it to the dotworkz housing. An additional bracket and clip were created to hold the Xavier NX within the housing. A 3D printed bracket or duct sealing putty is adequate to keep the light in place. Cabling includes power into each housing and Ethernet into

The OSCRE Imaging System

Considerations made for the camera and lens included affordability, flexibility, light sensitivity, and output capabilities. Machine vision cameras that incorporated Sony monochrome complementary metal oxide semiconductor (CMOS) sensors were selected due to noise/light performance, low exposure times, and use of a global shutter. The latter feature is particularly important for minimizing distortion caused by object motion during individual frames. The current generation of OSCRE uses a 3.2 MP FLIR BFS-UD32S4M-C camera with a Sony IMX252 sensor capable of a maximum framerate of 118 fps. Exact imaging properties such as resolution and field of view (FoV) are dependent on the matched lens and focal length chosen; this allows customization of the system to the observations desired (e.g., shattered blowing snow particles versus large aggregate snowflakes).

To minimize issues with distortion and ensure compatibility with future machine vision cameras (that have larger sensor sizes), a Rokinon 135 mm f/2 full-frame lens with manual aperture and focus controls was selected. Matched to the 1/1.8 inch Sony IMX252 sensor, the 135 mm lens acts as an effective 648 mm (4.8 \times crop factor) lens with a minimum focal length of 0.8 m. Distortion is $<0.02\%$ due to only the center of the lens being used. At a distance of 0.8 m, the FoV is 34 mm \times 26 mm resulting in 16.7 μ m pixels. A better balance of resolution and FoV occurs at longer focal lengths (e.g., 1.5 m). This increases FoV to 76 mm \times 57 mm and pixel size to 37 μ m. Depth of field (DoF) is also increased and is on the order of tens of millimeters (exact DoF is dependent on contrast detection of objects). Microscope test charts at a distance of 1.5 m suggest hydrometeors ~ 50 μ m can be identified, but with equally as large uncertainty due to specular reflection/contrast issues and fore/aft displacement of the hydrometeor.

The system is controlled by a NVIDIA Jetson graphics processing unit (GPU) computer. Initial development began with a Jetson TX2 contained within a heated, weatherproof box (Fig. 1b). The current device uses the Xavier NX developer kit, which is small enough to be included in the camera housing (Fig. 1b). The Ubuntu operating system is installed on a 32 GB microSD card while a 2 TB Solid State Drive (SSD) is used for recording data. This allows for continuous operation of the camera at a rate of 30 fps for ~ 6 h, although greater frame rates are possible if desired. Until real-time GPU-based software is developed, read/write performance is the single greatest factor on time and a quality SSD is required. The system can also be driven by other operating systems if desired; FLIR software runs on Linux, macOS, and Windows platforms.

the computer (although wireless can also be used). The most complex part of the system is 5–6 pin output wiring between the light, camera, and external power. This requires a pull-up resistor to activate the strobe with the output wire.

Example imagery. The 2019/20 winter was a perfect test period for OSCRE featuring a wide range of precipitation events from October to May. During this period, the system used a JAI 2.3 MP machine vision camera at a focal length of 0.8 m (Fig. 1a), yielding an effective resolution of $\sim 28 \mu\text{m}$ per pixel for the images shown in Figs. 2 and 3. Exposure times ranged from 6 to 10 μs at a rate of 30 frames per second (fps).

Multiple blizzards were sampled, including a Colorado low event with significant falling and blowing snow on 28–30 December 2019 and a ground blizzard forced by an Arctic front on 12 February 2020.¹ OSCRE images during blowing snow are characterized by a large number of ice crystals with maximum dimensions typically $< 1 \text{ mm}$ (Fig. 2). Although scenes were predominately shattered and rounded ice crystals (~ 100 were identified in Fig. 2a), larger hydrometeors were occasionally seen such as a 1.7 mm hexagonal plate (Fig. 2a) and a 4.4 mm broken dendrite (Fig. 2b). These images also demonstrate a limitation of the current lighting system; even with narrow optics, the lighted volume is deeper than the depth of field (DoF). This led to a large number of out of focus hydrometeors, necessitating image processing schemes that require contrast detection. Part of this issue was resolved by switching to a camera with a smaller sensor. This allows for equivalent resolution but at a longer focal length, nearly doubling the DoF.

Besides blizzards, OSCRE sampled a wide variety of snowfall and mixed-phase events (Fig. 3). On 15 December 2019, a light snow event occurred with a near-saturated, boundary layer temperature profile within the dendritic growth zone (DGZ, $-15^\circ \pm 5^\circ\text{C}$). Not surprisingly, snowflake habit featured a number of fern and stellar dendrites along with simple stars (Fig. 3a). Broken dendrites were also seen along with growth around rimed cores. Some aggregation was observed, with the largest $\sim 1 \text{ cm}$ in length. Note that the singular viewing angle for OSCRE (unlike MASC) can occasionally lead to needle-like shapes due to snowflakes being imaged parallel to their primary face.

Prior to blizzard conditions being reached during the 12 February 2020 event, OSCRE sampled prefrontal snow (Fig. 3b). Conditions during this period were much warmer with lack of a DGZ. Habit was predominately irregular aggregates with various extents of riming. In the 30 min leading up to the frontal passage at $\sim 0730 \text{ UTC}$, there was a noticeable change in habit to fewer aggregates and more rimed snowflakes.

The final highlighted event is a mixed-phase event on 2 April 2020 (Fig. 3c). With conditions near freezing, the event started with a variety of hydrometeors at the surface including rain

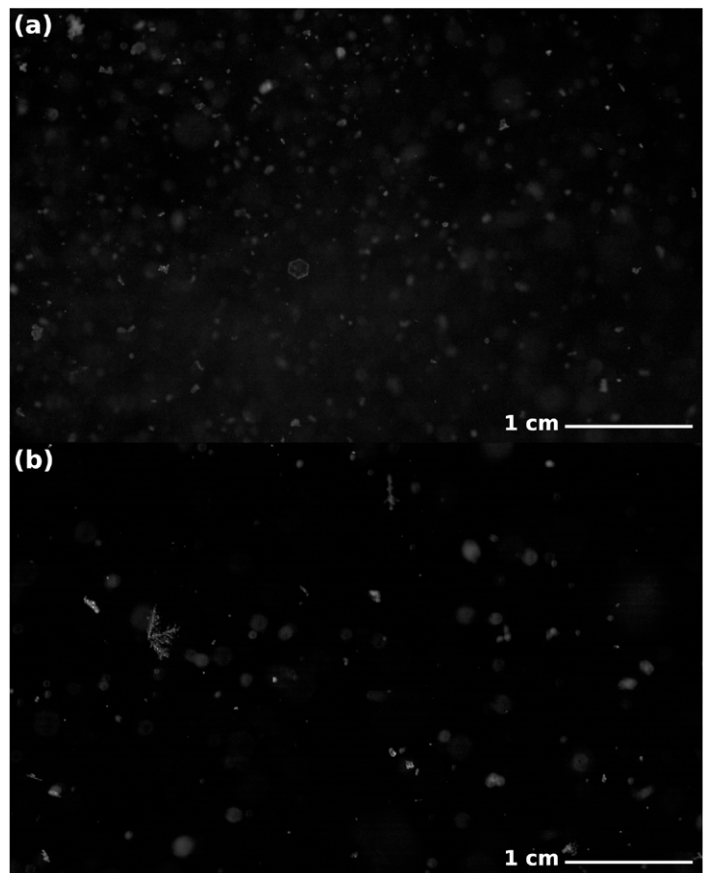


Fig. 2. Singular frames from OSCRE during blizzards. Images are valid at (a) 1630 UTC 29 Dec 2019 and (b) 1010 UTC 12 Feb 2020.

¹ Descriptions of these blizzard causing systems are provided in Kennedy et al. (2019).

(3 dotted structures due to reflection/refraction of light), partially and fully frozen drops including spicules, and melted snowflake structures. As the event progressed, there was a rapid change to large aggregates, with the largest having a maximum diameter > 4 cm (this structure extended out of frame). The duration of large aggregates was short lived, with later habits featuring smaller aggregates and individual snowflakes with riming.

BLOWN-UNDER: Students lead the way

BLOWN-UNDER took lessons learned from the first author during their experience as a graduate student associated with the Student Nowcasting and Observations of Winter Weather with the DOW at University of North Dakota Education in Research (SNOWD UNDER) campaign held in 2010 (UCAR 2020). Similarly, BLOWN-UNDER was designed by students. An initial kick-off meeting identified goals and broke the project into five teams (Table 2). Each team was led by a graduate student and appropriate operations and safety plans were created. This provided structure to the campaign, gave graduate students leadership experience, and facilitated communication throughout the group. Undergraduate and other interested graduate students were assigned to groups based on interest. The project involved five graduate student leaders and an additional 19 undergraduates and graduate students assigned to teams. A few additional individuals assisted with other aspects of the campaign such as educational outreach and the 12 February 2020 IOP.

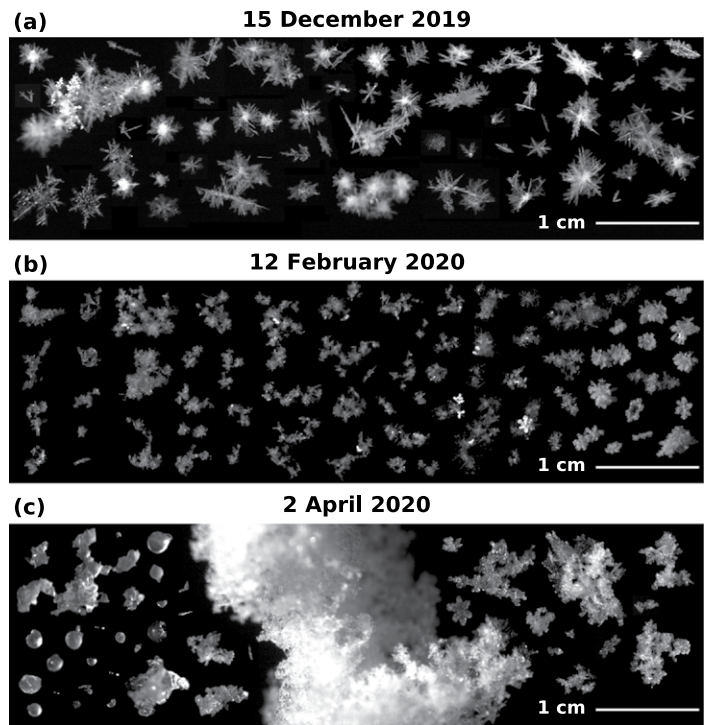


Fig. 3. Composite images from OSCRE for (a) 1500–2000 UTC 15 Dec 2019, (b) 0500–0730 UTC 12 Feb 2020, and (c) 1230–1330 UTC 2 Apr 2020. Images are arranged in approximate chronological order with earlier times on the left.

Table 2. BLOWN-UNDER teams and respective learning goals, responsibilities, and instrumentation.

Team	Learning goals and responsibilities	Instrumentation
Surface	Learn about and operate in situ and remotely sensed surface instruments. Maintain field site and keep instruments operational at the Oakville Prairie Observatory.	Lufft CHM-15K ceilometer NDAWN Mesonet OSCRE Parsivel ²
Balloon	Learn how to launch traditional and PASIV balloon packages. Assist with tracking and retrieval of PASIV launches.	GRAW DFM-09 radiosondes PASIV
Radar	Learn about dual-polarimetric radar observations and scanning strategies. Coordinate and operate UND and DOW7 radars.	DOW7 (X-band) Mayville, ND WSR-88D (S-band) UND North-Pol (C-band)
Forecasting	Learn about numerical weather prediction. Gain hands-on experience running WRF and interpreting output from operational models. Provide weather briefings for the project and real-time guidance to the group.	
Media	Learn about reporting and gain video editing experience. Coordinate social media posts and disseminate info to other news agencies.	

Science goals and observations during blizzard events. The primary science goals of the campaign were to characterize micro- and macrophysical properties and boundary layer structure and evolution during blizzard and blowing snow events. The strengths and weaknesses of deployed instruments (including OSCRE) were also explored to guide future field work. A list of instruments partitioned by team is provided in Table 2.

Surface instrumentation included standard meteorological observations from a mesonet site and DOW7, and microphysical information from an OTT Hydromet Parsivel² and the OSCRE. The latter two instruments were deployed to provide microphysical ground truth (PSDs) and to help segregate between falling/blowing snow. A loaned North Dakota Agricultural Network mesonet with a 3 m tower was collocated with the ceilometer and Parsivel² at the Oakville Prairie Observatory located ~13 mi west of Grand Forks, North Dakota, near the Grand Forks Air Force Base. Limited bandwidth at this location along with the experimental nature of OSCRE led to deployment of this instrument within Grand Forks, North Dakota.

Remotely sensed observations included both radar and lidar assets. A Lufft CHM 15k 1,064 nm laser ceilometer was loaned to the project from OTT Hydromet. Providing vertical profiles of attenuated backscatter, deployment allowed for surface-based detection of blowing snow layers similar to studies in Antarctica (Gossart et al. 2017; Loeb and Kennedy 2021).

Core instrumentation such as the ceilometer sampled blowing snow layers during several blizzards to varying degrees of success (Fig. 4). During and after an extended period of falling snow, blizzard conditions were reached from 1500 to 0200 UTC 29–30 December 2019 (Fig. 4a). Blowing snow is easily identified by the near-surface maximum of backscatter throughout the period with layer heights around 300–400 m. Fall streaks and cloud structures above the blowing snow layer were also present suggesting the ceilometer was not significantly attenuated by the blowing snow.

Greater measurement difficulty for the ceilometer was found with the 12 February 2020 ground blizzard (Fig. 4b). Meteorologically, this event was forced by an intense Arctic front. Over the course of minutes, wind magnitude increased from 7 to 20 m s⁻¹. The strong winds combined with recent prefrontal snowfall led to a wall of darkness (whiteout

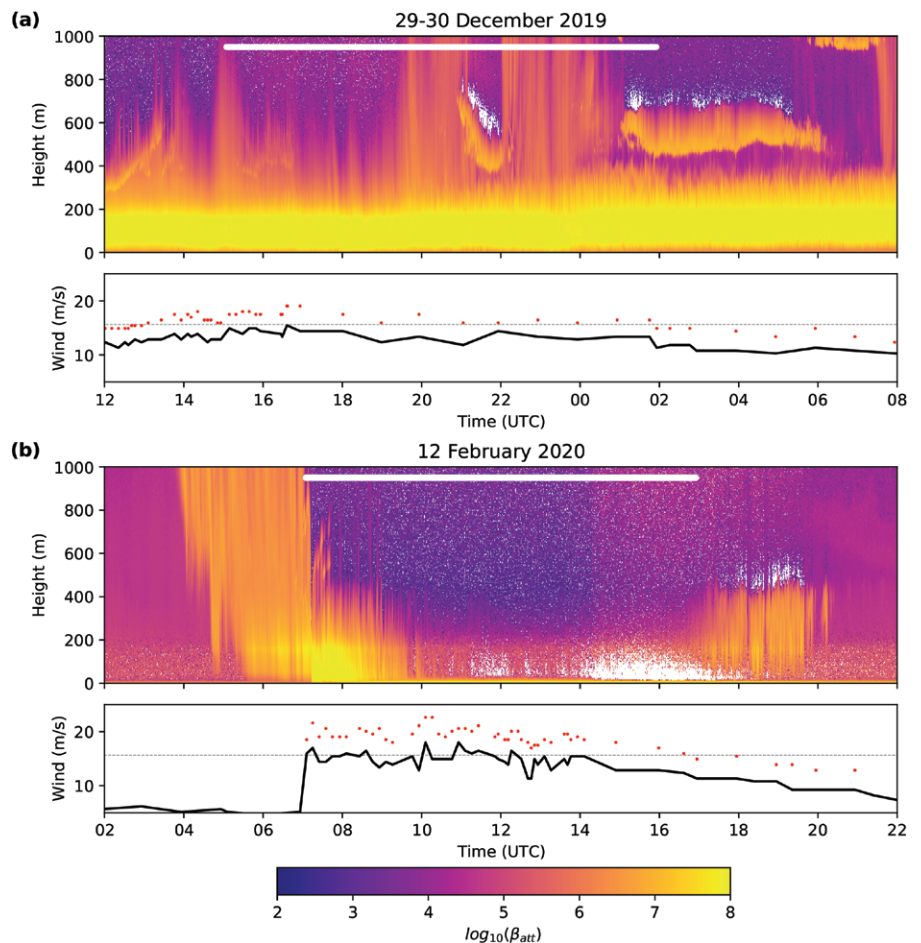


Fig. 4. Time series plots of attenuated backscatter from the Lufft CHM 15K ceilometer at the Oakville Prairie Observatory and measured 10 m winds at the nearby Grand Forks Air Force Base (KRDR) for blizzard events on (a) 29–30 Dec 2019 and (b) 12 Feb 2020. White bars indicate time periods with visibility < 0.5 mi at KRDR. Sustained winds are plotted with black solid lines with wind gusts given by red markers. The dashed gray lines represent the threshold wind speed (15.6 m s⁻¹ or 35 mph) for blizzard conditions.

conditions) as seen by area cameras (not shown). This frontal passage is easily seen in the ceilometer data by a rapid increase in backscatter in the lower 200 m of the profile at 0715 UTC. After a couple of hours of intense near-surface backscatter extending up to ~500 m, the blizzard was strong enough to limit penetration to only the lowest several range bins (<50 m). Blowing snow layer heights were only retrievable as the event subsided (1700 UTC). In this and other cases, temporal fluctuations in ceilometer backscatter were present, indicative of horizontal convective rolls containing blowing snow (Kennedy and Jones 2020). Further, most events concluded with backscatter first diminishing near the surface as winds decreased, and then a gradual reduction of intensity within a suspended blowing snow layer.

Radars are also capable of detecting blowing snow events (Vali et al. 2012; Geerts et al. 2015; Kennedy and Jones 2020; Loeb and Kennedy 2021), although exact sensitivity limits are unknown. To provide mesoscale details and understand detection limits, dual polarized observations were made at X (DOW7, <https://dowfacility.atmos.illinois.edu/>), C (UND NorthPOL, <http://radar.atmos.und.edu/>), and S (KMXV WSR-88D, <https://www.roc.noaa.gov/WSR88D/>) bands. Scanning strategies between DOW7 and NorthPOL were coordinated during the 12 February 2020 blizzard including synced scans between the radars. Deployment locations for DOW7 were identified in advance to minimize issues with beam blockage and allow for Dual-Doppler lobes with either NorthPOL or KMXV.

Example radar data from 0840 UTC during the 12 February 2020 blizzard are provided in Fig. 5. The location of the front (now south of the campaign location) is seen as a fine line in KMXV data (Fig. 5c). Immediately behind the prefrontal snow and cold front are horizontal convective rolls of blowing snow near DOW7 and KMXV (Figs. 5a,c). Oriented approximately north to south with the mean boundary layer wind vector, these shallow features are associated with increased reflectivity and variability in the velocity field (not shown). As the event progressed, these features took on an elongated and more regularly spaced appearance typical of other events (Kennedy and Jones 2020). While falling snow was also viewed by NorthPOL, clutter issues in the lowest layers (within city limits) prevented detection of the horizontal convective rolls (Fig. 5b). The shallow nature of the blowing snow layer (~400–500 m as detected by radar) means that detection was limited to tens of kilometers from radar sites at the lowest usable elevation tilts.

Two types of sondes were launched during BLOWN-UNDER with GRAW DFM-09 radiosondes providing wind, temperature, humidity, and pressure observations while the PASIV provided vertical profiles of PSDs (Fig. 6). The campaign used an upgraded version of the first generation PASIV (Waugh et al. 2015).

The new version uses a 4112×3008 pixel Ximea MC124CG-SY machine vision camera powered by an Nvidia Jetson TX2 computer. With a sampling volume of $29 \text{ cm} \times 20 \text{ cm} \times 11.5 \text{ cm}$, the system is capable of resolving hydrometeors $> 100 \mu\text{m}$ in diameter at a rate of ~20 frames per second. The weight of the PASIV (just under the U.S. Federal Aviation Administration regulation Part 101 limit of 2.72 kg) necessitated a large amount of helium (two

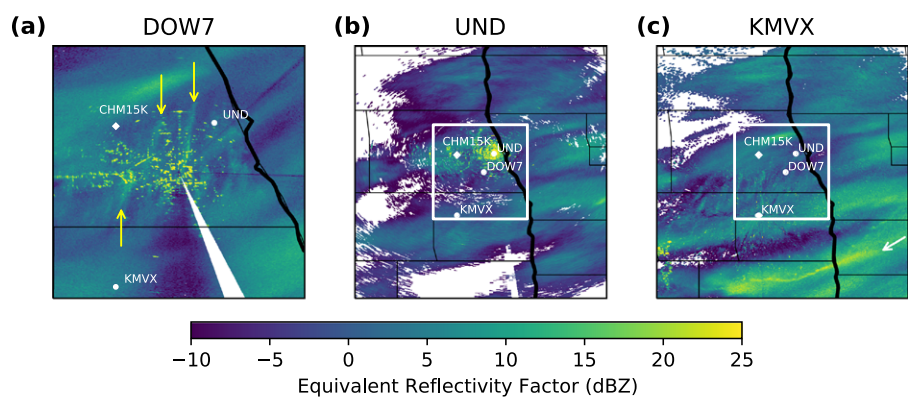


Fig. 5. Reflectivity PPIs valid at 0840 UTC 12 Feb 2020 for (a) DOW7 (1.3°), (b) UND (2.0°), and (c) KMXV (0.5°). DOW7 is plotted as a geographical subset as indicated by the white box. Horizontal convective rolls in the DOW7 panel are denoted by yellow arrows, while the fine line associated with the Arctic front is identified by the white arrow in the KMXV panel. CHM15K is the location of the ceilometer shown in Fig. 4b.

200 HE cylinders; 11.3 m^3) per launch. Due to a regional helium shortage during the campaign, only two launches were made (6 and 12 February 2020). Because the PASIV does not actively transmit data, probes were retrieved with aid of a SPOT GPS tracker (Figs. 6b,c).

Ballooning is notorious for adventures, and BLOWN-UNDER was no exception. The 6 February 2020 launch did not use a cut-down mechanism and traveled far enough to land in a forested recreational area near Fertile, Minnesota (Fig. 6b). Unfortunately, the data disk became loose during launch and no hydrometeor information was recorded. Issues with the cut-down device and security of the drive were fixed by 12 February 2020, and a launch in prefrontal snow was made at 0640 UTC. Given the close proximity of recovery and expected winds behind the front, the decision was made to retrieve the device prior to the frontal passage. While this was achieved (Fig. 6c), retrieval was delayed due to the need to snowshoe into a field. On the way back to town, the recovery team including the first author was hit by the frontal passage and ended up stuck in open country until conditions improved $\sim 8 \text{ h}$ later. An important safety lesson was learned, but PASIV data were successfully recovered (Fig. 6d).

Communications. Communications for the project varied before and during the DOW7 deployment window. Leading up to the campaign, communications were traditional, using email and surveys to build teams and schedule meetings. During the IOP period, communication was maintained using daily weather briefings and the popular, freeware

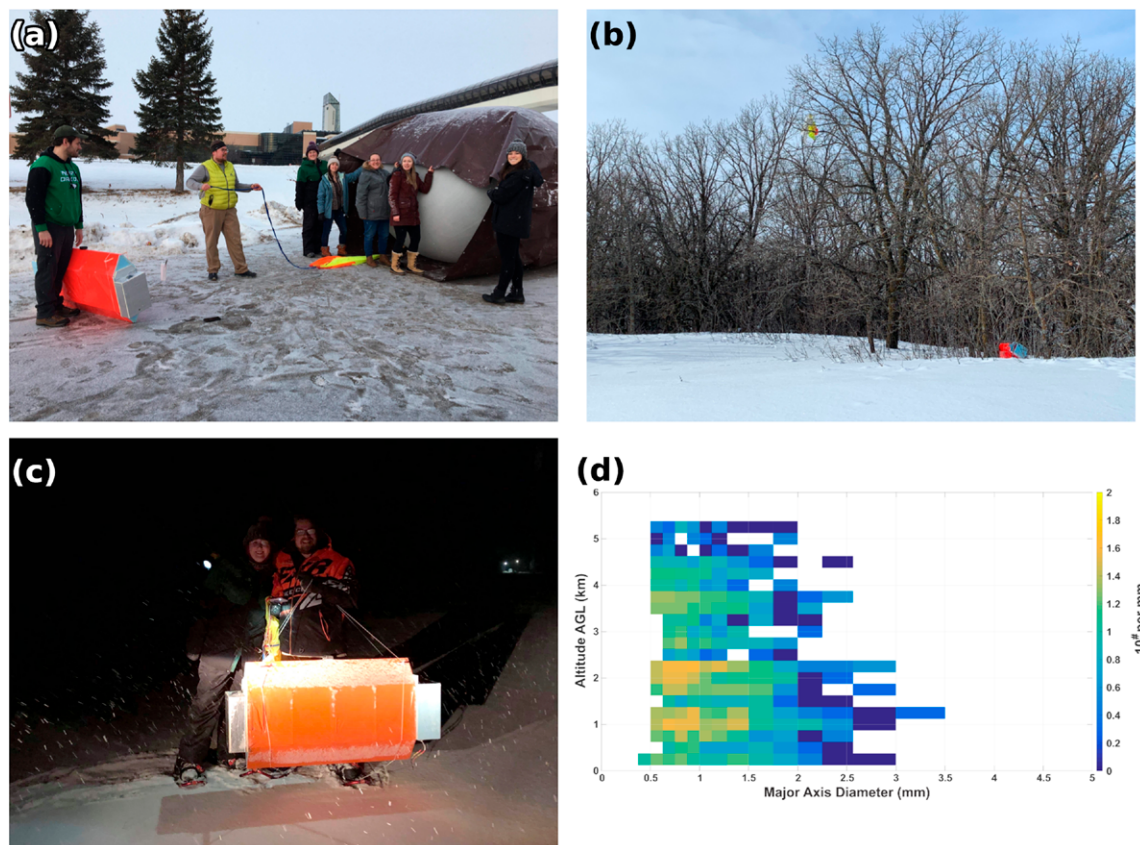


Fig. 6. PASIV launches during BLOWN-UNDER. (a) The initial launch is prepared during a light snow event on 6 Feb 2020. From left to right: Alec Sczepanski, Aaron Kennedy, Julianna Glinskas, Caitlyn Mensch, Nikki Carson-Marquis, Nicole Loeb, and Elizabeth Sims. (b) The 6 Feb 2020 launch is recovered within the Sand Hill River Recreation Area near Fertile, Minnesota, on the same day. (c) The 12 Feb 2020 launch is recovered by Julianna Glinskas, Aaron Kennedy, and Nicole Loeb (photographer) from a field near Key West, Minnesota, prior to the onset of blizzard conditions. (d) The vertical profile of major axis diameter (mm) from the 12 Feb 2020 launch.

instant messaging application, Discord (Fig. 7). While the use of Discord has been noted in educational environments (Lacher and Biehl 2018; Fonseca Cacho 2020), the authors are unaware of formal publications documenting use of Discord for field campaigns.

Highlighting the use of Discord, this activity was considered a success. The ability to create multiple channels to support specific teams decluttered communications. Support for pictures and videos was extensively used to share real-time data (e.g., DOW7 and sounding data). Finally, instant messaging was used to contact specific users. Because Discord is supported in web browsers as well as OS specific applications, it was easily accessible to campaign participants. While not used, the ability to program bots could be advantageous in the future (e.g., querying real-time data from observations). While virtually all of these features are also available in the Slack platform, it is worth noting that Discord is more commonly used by students due to its presence in online gaming communities.

Forecast and modeling activities. Local noon (1800 UTC) weather briefings were prepared by the student forecasting team each weekday of the campaign. Students met to view real-time observations and model output to produce a forecast for the next 3 days. If the possibility of falling or blowing snow was identified, the entire team was put on alert and additional times (e.g., the weekend) were identified for team members to be on call. During IOPs, team members kept others updated on conditions via Discord.

Besides the standard suite of operational models, forecasters also had access to Weather Research and Forecasting (WRF) Model simulations designed by the team. These simulations were run daily at 0000 and 1200 UTC on a local cluster. Students prioritized resolution and chose a 3 km inner nest, and output was tailored to the project including appropriate variables (visibility) from the Air Force Weather Agency (AFWA) and contouring intervals appropriate for the time period. To show the absence of blowing snow in WRF and its impacts on forecast visibility, a column blowing snow model, PIEKTUK (Déry and Yau 2001), was implemented in Python and forced by WRF output.

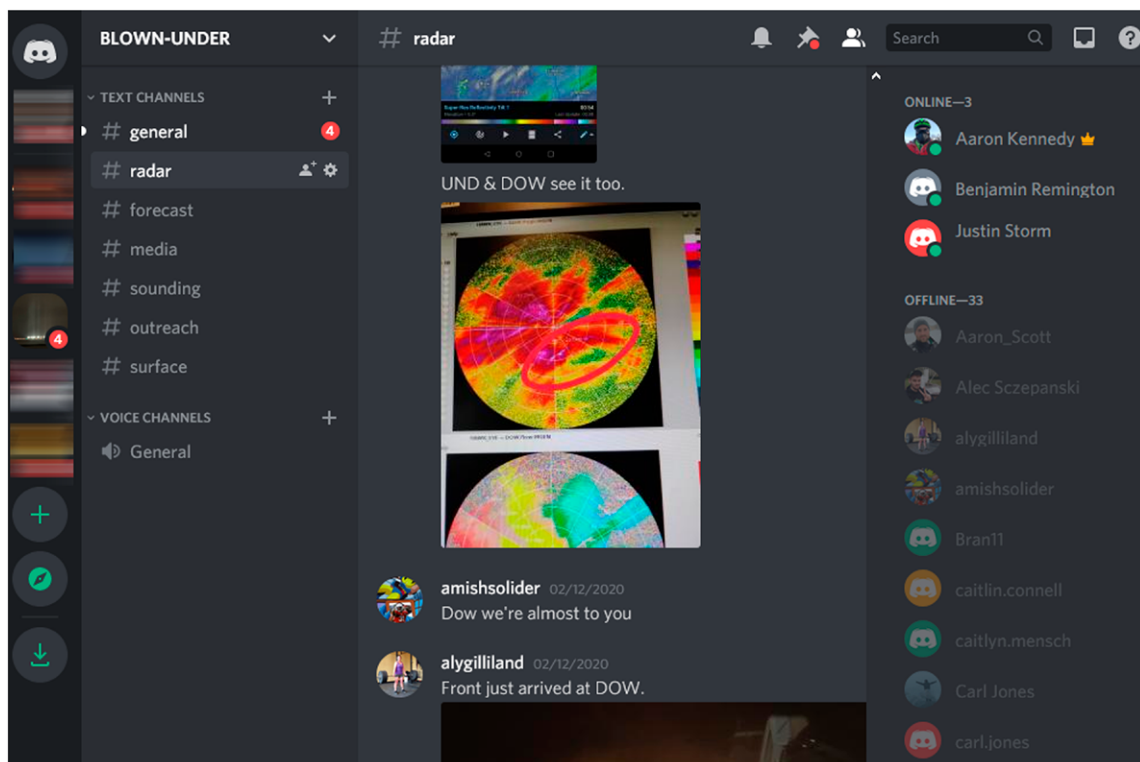


Fig. 7. Example of Discord use within the #radar subchannel during the 12 Feb 2020 blizzard event.

Observation based analyses and WRF output valid at 0900 UTC 12 February 2020 during the ground blizzard component of the event are shown in Fig. 8. The location of the southward moving Arctic front is easily identifiable by the gradient in temperature, and presence of strong northerly winds behind the front (Figs. 8a,b). Visibility reductions due to falling snow were present along the front in both observations and WRF AFWA output (Figs. 8a,c). More significant reductions in visibility occurred behind the front due to blowing snow; the lack of this process in WRF led to no reductions in visibility for this region (Fig. 8c). PIEKTUK on the other hand, showed reduced visibilities behind the front where wind speeds were sufficiently strong to trigger the column blowing snow model (Fig. 8d). While this is an encouraging result, it is noted that impacts were too widespread. In this case, blowing snow did not occur where little to no snow fell leading up the frontal passage. This highlights the ongoing work needed to improve blowing snow modeling before it is widely included within mesoscale models.

Connecting research to outreach

The widespread impacts of winter weather on the northern Great Plains make the subject a perfect topic for outreach. A number of activities were carried out before and during the BLOWN-UNDER campaign. Approximately 1,000 individuals were reached during the 2019/20 winter across a tribal college outreach program, a STEM café at a local brewery, school visits, and science/community days in the region (Table 3). The quiescent start to the campaign

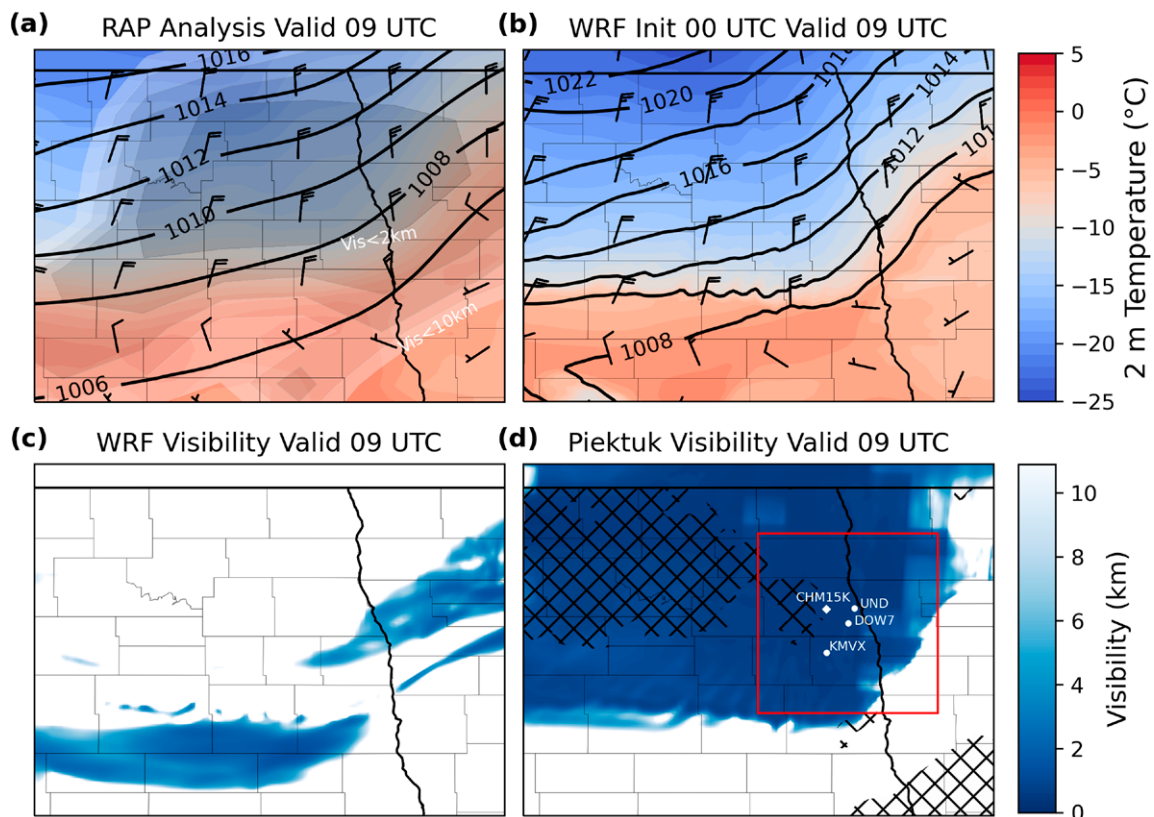


Fig. 8. Analysis and forecast of 2 m temperature ($^{\circ}\text{C}$), mean sea level pressure (hPa), 10 m winds (m s^{-1}), and visibility (km) valid at 0900 UTC 12 Feb 2020. (a) RAP analysis with observed visibilities contoured with gray shading. (b) WRF 9 h forecast initialized at 00 UTC 12 Feb 2020. (c) WRF AFWA visibility (km). (d) Piektuk blowing snow visibility (km) initialized from WRF output. The hatching in (d) indicates regions without recent snowfall (72 h prior) as identified from the NOAA National Snow Analyses produced by the National Operational Hydrologic Remote Sensing Center. The red box in (d) indicates the area shown in Figs. 5b and 5c.

Table 3. BLOWN-UNDER outreach events and attendance.

Event	Date	Total	Adults	Kids			Underrepresented	Special needs	General public
				Total	Male	Female			
NATURE	Various	81	5	76	NA	NA	82	0	0
Hopped up On Science @ Half Brothers Brewing	22 Jan 2020	40	36	4	1	3	NA	NA	40
Holy Family / St Mary's Elementary School	23 Jan 2020	75	6	69	40	29	3	0	6
Thompson K-12	28 Jan 2020	13	1	12	9	3	1	0	1
Sacred Heart K-12	30 Jan 2020	14	3	11	7	3	2	0	3
Little Hoop Tribal Community College	2 Feb 2020	31	31	NA	NA	NA	31	NA	11
Grand Forks Central High School	5 Feb 2020	152	6	146	80	61	36	10	6
Aerospace Community Day (hands-on)	8 Feb 2020	511	237	274	NA	NA	NA	NA	NA
Discovery Elementary School	11 Feb 2020	82	4	78	35	43	9	2	4
Total (All)		999	330	670	187	164	168	12	106

allowed for more visits with DOW7 than otherwise expected, and one day was set aside for the radar to visit the Little Hoop Tribal Community College within the Spirit Lake Reservation.

A core component of outreach was the development of hands-on activities to engage participants (Fig. 9). Learning objectives included discovery of snow properties, identifying whether it can be blown, and understanding how light interacts with ice crystals. Several of these activities are now described.

Blizzard in a box. Two types of artificial snow were acquired including finely ground plastic shavings and a water absorbent polymer. These represent snowfall events with low and high liquid water content, respectively. After students felt each type of snow, they were encouraged to think about how this impacts real-world experiences such as creating snowballs or shoveling snow. They were then asked which one is more likely to be blown by the wind. A handheld fan was then used to (unsuccessfully) blow the wet snow. The activity then shifted to an aquarium that held the dry, plastic-based artificial snow (Fig. 9a). Participants created LEGO creations to serve as obstacles. With the tank mostly covered, students then used the handheld fan to create a blizzard. After the wind subsided, students were asked about snow drifts and how this impacts the measurement of snowfall. Depending on the age level, this activity was a qualitative or quantitative exercise, but the end result was a better understanding of how obstacles and drifts impact snowfall measurements.

Atmospheric optics. Sun dogs, light pillars, and other more complex halos are a common occurrence in the region. To teach individuals about the concepts of reflection and refraction, 3D printed hexagonal plate crystals were created with a resin 3D printer (Fig. 9b). After the crystals were printed, they were sanded down to 2,000-grit, then coated in clear automotive enamel. The result is an almost completely transparent, custom made prism. Students used a flashlight to see the processes of refraction and reflection. In practice, the crystals will reflect light upward or downward off the face (responsible for light pillars) and refract light at an angle to produce sun dogs (parhelia).



Fig. 9. Examples of hands-on outreach activities: (a) blizzard in a box, (b) atmospheric optics with a custom hexagonal ice crystal, (c) snowflake habit matching, and (d) snowflake art.

Snowflake habit matching and art. Three-dimensional printers were used to create specific snowflake habits (plates, aggregates, bullet rosettes, columns, etc.) to teach individuals about the variability of ice habits and environments they form in (Figs. 9c,d). Printed crystals were matched to a graphic table of habits, and real-world examples were shown from OSCRE. A Thingiverse project (The Snowflake Machine by user mathgrrl) was used to create randomly generated dendrites. These were handed out to students to use for art rubbings and were allowed to be taken home as gifts.

Hands-on activities were also packaged into a complete winter weather module for the Nurturing American Tribal Undergraduate Research and Education (NATURE) Sunday Academy outreach program. The authors traveled to five tribal colleges throughout the fall and winter and presented to high school students at their respective reservations. Topics of the unit included a cultural connection activity (e.g., a history of winter counts) taught by a tribal liaison, and various winter weather lessons ranging from winter safety tips to reading weather maps and identifying the type of weather systems responsible for blizzards in the region. Hands-on activities were mixed throughout the lesson to provide engagement. Formal assessment for the program was positive with a mean rating of 3.87 out of 5.0 (with 1 = poor, 5 = excellent) for overall quality of the lesson. Other questions asked about how interesting the topic was (3.76), the extent hands-on activities added to lesson quality (3.09), and the extent to which Native American culture and the science topic were related (2.85). Students highlighted the hands-on activities, and suggestions for improvement included adding more of these activities. To improve the cultural connection score, future iterations should mix these activities throughout the event versus having a stand-alone section at the beginning.

Summary and lessons learned.

While blizzards are common in the region, there is no guarantee weather will cooperate for field campaigns, especially those with short time windows such as educational deployments. An active winter ensured OSCRE had plenty of events to sample throughout the winter, but most of the BLOWN-UNDER IOP period was quiet. This time was instead used to exceed expectations for outreach. Regarding science objectives, the ground blizzard of 12 February 2020 was a home-run event by every measure, ensuring these goals were also met. The combination of in situ and remotely sensed observations of the event will offer an unprecedented look into the evolution of a ground blizzard, and a detailed case study is the subject of forthcoming work.

Moving forward, a number of lessons were learned that will guide future deployments for blizzard research. Regarding observations during BLOWN-UNDER:

- Importance of winterizing equipment: While DOW7 performed admirably for the event, exposure and cold took its toll as blowing snow was ingested into various components of the system, eventually leading to failure of the generator powering the radar. The cold also led to the hydraulic mast freezing, leaving DOW7 in place until it could be loosened (Fig. 10).
- The dynamic landscape of cold regions: While deployment locations were scouted in advance for DOW7, anthropogenic piles of snow and natural drifts led to surprises. Time must be set aside prior to events to identify ideal locations for mobile assets.
- The difficulty and safety of PASIV launches. The weight of the current PASIV necessitates a large balloon that uses two size 200 cylinders of helium. This weight is still sufficiently light with a large surface area that makes launches in windy environments challenging (e.g., the instrument can be difficult to hold in high winds). Weight savings can be sought to reduce the overall size of the instrument and thus reduce the complexity in launching. Additionally, a reduction in weight would also reduce the helium required for lift. Further, the PASIV can be modified for missions that are focused on the near-boundary layer, maximizing the residence time in the region of interest rather than the entire troposphere as originally designed. Finally, key components should be ruggedized so there is no need or desire to retrieve probes immediately. This will ensure the safety of participants as launches can be made near heated locations where cold exposure is kept to a minimum. Participants that help with retrievals after events conclude should be provided training regarding cold weather attire and retrieval methods such as snowshoeing.

Regarding the development and deployment of OSCRE:



Fig. 10. Undergraduate student Justin Storm walks away from DOW7 as the 12 Feb 2020 ground blizzard comes to an end. Picture taken by undergraduate student Caitlin Connell.

- Feasibility of affordable microphysical measurements: OSCRE has demonstrated that habit and size can be obtained in nearly any cold-season environment. The price point is significantly less than commercial options suggesting networks could be implemented to understand spatial and temporal variability of falling and blowing snow.
- Computing limitations: Making OSCRE affordable necessitated a number of design sacrifices such as brute-force imaging and off-the-shelf components. Current hardware does not support retrieval of fall speeds, but affordable advancements in cameras and computing may make this possible in the future. In its present form, OSCRE is capable of handling IOP style deployments, but long-term, unattended use will be possible with further code development.
- Lighting: Current lighting is sufficient for imaging hydrometeors but the sampling volume may be impacted by flow around the instrument. Current lighting has too much spread and this leads to the use of contrast-detection methods to identify in-focus hydrometeors. The lighting system needs further refinement to let the light define the sampling volume. This will simplify hydrometeor detection and may make analysis of hydrometeors feasible in real time. A housing could be developed to minimize flow disruptions and increase the intensity of light, but this will most likely increase the costs of the system.

Acknowledgments. BLOWN-UNDER was possible due to the support of numerous groups. Funding for the project and outreach efforts was provided by the National Science Foundation (NSF) under AGS 1834748 and NSF EPSCoR Track-1 Cooperative Agreement OIA 1355466. NSF support also included deployment of DOW7 through the NCAR Earth Observing Laboratory (EOL) educational deployment program. The authors thank Joshua Wurman, Karen Kosiba, and radar operator Alycia Gilliland of the Center for Severe Weather Research for their tireless support throughout the campaign. Other individuals that deserve recognition include Victor Cassella of OTT Hydromet who made the ceilometer deployment possible, Steve Kinney of Smart Vision Lights who provided helpful tips on machine vision lighting, and Daryl Richardson and James Hyde of the North Dakota Agricultural Network for loaning the mesonet station. The UND Departments of Biology and Space Studies are thanked for allowing use of the Oakville Prairie Field Station and Observatory. Finally, we thank three anonymous reviewers who provided feedback that improved the clarity of this manuscript.

Data availability statement. Code and data used to create figures within this manuscript along with OSCRE documentation are available at <https://github.com/KennedyClouds>.

Appendix: Acronyms

Acronyms used in the text are listed here.

2DVD	2D video disdrometer
AFWA	Air Force Weather Agency
BLOWN-UNDER	Blowing Snow Observations at the University of North Dakota: Education through Research
CMOS	Complementary metal oxide semiconductor
CPI	Cloud Particle Imager
DoF	Depth of field
DOW	Doppler on Wheels
DGZ	Dendritic growth zone
FoV	Field of view
GPU	Graphics processing unit
IOP	Intensive operation phase
MASC	Multi-Angle Snowflake Camera

NATURE	Nurturing American Tribal Undergraduate Research and Education
OSCRE	Open Snowflake Camera for Research and Education
Parsivel ²	Particle size velocity disdrometer
PASIV	Particle Size and Velocity probe
PIP	Precipitation Imaging Package
PSD	Particle size distribution
SNOWD UNDER	Student Nowcasting and Observations of Winter Weather with the DOW at University of North Dakota Education in Research
SPC	Snow-particle counter
SSD	Solid State Drive
SVI	Snow Video Imager
WRF	Weather Research and Forecasting

References

- Baggaley, D. G., and J. M. Hanesiak, 2005: An empirical blowing snow forecast technique for the Canadian Arctic and the Prairie Provinces. *Wea. Forecasting*, **20**, 51–62, <https://doi.org/10.1175/WAF-833.1>.
- Battaglia, A., E. Rustemeier, A. Tokay, U. Blahak, and C. Simmer, 2010: PARSIVEL snow observations: A critical assessment. *J. Atmos. Oceanic Technol.*, **27**, 333–344, <https://doi.org/10.1175/2009JTECHA1332.1>.
- Boustead, B. E., 2014: The Hard Winter of 1880–1881: Climatological context and communication via a Laura Ingalls Wilder narrative. Ph.D. dissertation, School of Natural Resource, University of Nebraska–Lincoln, 196 pp.
- , M. D. Shulski, and S. D. Hilberg, 2020: The long winter of 1880/81. *Bull. Amer. Meteor. Soc.*, **101**, E797–E813, <https://doi.org/10.1175/BAMS-D-19-0014.1>.

- Chritin, V., R. Bolognesi, and H. Gubler, 1999: FlowCapt: A new acoustic sensor to measure snowdrift and wind velocity for avalanche forecasting. *Cold Reg. Sci. Technol.*, **30**, 125–133, [https://doi.org/10.1016/S0165-232X\(99\)00012-9](https://doi.org/10.1016/S0165-232X(99)00012-9).
- Déry S. J., and M. K. Yau, 2001: Simulation of blowing snow in the Canadian arctic using a double-moment model. *Bound.-Layer Meteor.*, **99**, 297–316.
- Fitch, K. E., C. Hang, A. Talaei, and T. J. Garrett, 2021: Arctic observations and numerical simulations of surface wind effects on Multi-Angle Snowflake Camera measurements. *Atmos. Meas. Tech.*, **14**, 1127–1142, <https://doi.org/10.5194/amt-14-1127-2021>.
- Fonseca Cacho, J., 2020: Using discord to improve student communication, engagement, and performance. UNLV Best Teaching Practices Expo, 95, https://digitalscholarship.unlv.edu/btp_expo/95.
- Garrett, T. J., C. Fallgatter, K. Shkurko, and D. Howlett, 2012: Fallspeed measurement and high-resolution multi-angle photography of hydrometeors in freefall. *Atmos. Meas. Tech.*, **5**, 2625–2633, <https://doi.org/10.5194/amt-5-2625-2012>.
- Geerts, B., B. Pokharel, and D. A. R. Kristovich, 2015: Blowing snow as a natural glaciogenic cloud seeding mechanism. *Mon. Wea. Rev.*, **143**, 5017–5033, <https://doi.org/10.1175/MWR-D-15-0241.1>.
- Gossart, A., N. Souverijns, I. V. Gorodetskaya, S. Lhermitte, J. T. M. Lenaerts, and J. H. Schween, 2017: Blowing snow detection from ground-based ceilometers: Application to East Antarctica. *Cryosphere*, **11**, 2755–2772, <https://doi.org/10.5194/tc-11-2755-2017>.
- Green, C., and R. Thornton, Eds., 2007: *The Year the Stars Fell: Lakota Winter Counts at the Smithsonian*. University of Nebraska Press, 370 pp.
- Howe, C., 2015: Lakota star knowledge and Lakota winter counts. Lecture presented at Oglala Lakota College, 12 November 2015, <https://www.youtube.com/watch?v=TEyJraivn8M>.
- Kapela, A. F., P. W. Leftwich, and R. Van Ess, 1995: Forecasting the impacts of strong wintertime post-cold front winds in the northern plains. *Wea. Forecasting*, **10**, 229–244, [https://doi.org/10.1175/1520-0434\(1995\)010<0229:FTIOSW>2.0.CO;2](https://doi.org/10.1175/1520-0434(1995)010<0229:FTIOSW>2.0.CO;2).
- Kennedy, A., and C. Jones, 2020: GOES-16 observations of slowing snow in horizontal convective rolls on 24 February 2019. *Mon. Wea. Rev.*, **148**, 1737–1750, <https://doi.org/10.1175/MWR-D-19-0354.1>.
- , A. Trellinger, T. Grafenauer, and G. Gust, 2019: A climatology of atmospheric patterns associated with Red River valley blizzards. *Climate*, **7**, 66, <https://doi.org/10.3390/cli7050066>.
- Kremer, K. 2015, *Angel of the Prairie: The Heroic Story of Hazel Miner During the North Dakota Blizzard of 1920*. Snow in Sarasota Publishing, 125 pp.
- Kumjian, M. R., K. A. Bowley, P. M. Markowski, K. Lombardo, Z. J. Lebo, and P. Kollias, 2020: Snowflake selfies: A low-cost, high-impact approach toward student engagement in scientific research (with their smartphones). *Bull. Amer. Meteor. Soc.*, **101**, E917–E935, <https://doi.org/10.1175/BAMS-D-19-0096.1>.
- Lacher, L., and C. Biehl, 2018: Using discord to understand and moderate collaboration and teamwork. *Proc. 49th ACM Technical Symp. on Computer Science Education*, Baltimore, MD, Association for Computing Machinery, 1107, <https://doi.org/10.1145/3159450.3162231>.
- Laskin, D., 2005: *The Children's Blizzard*. 3rd ed. HarperCollins, 336 pp.
- Lawson, R. P., B. A. Baker, C. G. Schmitt, and T. L. Jensen, 2001: An overview of microphysical properties of Arctic clouds observed in May and July during FIRE.ACE. *J. Geophys. Res.*, **106**, 14 989–15 014, <https://doi.org/10.1029/2000JD900789>.
- , ——, P. Zmarzly, D. O'Connor, Q. Mo, J.-F. Gayet, and V. Shcherbakov, 2006: Microphysical and optical properties of atmospheric ice crystals at South Pole Station. *J. Appl. Meteor. Climatol.*, **45**, 1505–1524, <https://doi.org/10.1175/JAM2421.1>.
- Li, L., and J. W. Pomeroy, 1997a: Estimates of threshold wind speeds for snow transport using meteorology data. *J. Appl. Meteor.*, **36**, 205–213, [https://doi.org/10.1175/1520-0450\(1997\)036<0205:EOTWSF>2.0.CO;2](https://doi.org/10.1175/1520-0450(1997)036<0205:EOTWSF>2.0.CO;2).
- , and ——, 1997b: Probability of occurrence of blowing snow. *J. Geophys. Res.*, **102**, 21 955–21 964, <https://doi.org/10.1029/97JD01522>.
- Loeb, N. and A. Kennedy, 2021: Blowing snow at McMurdo Station, Antarctica During the AWARE field campaign: Surface and ceilometer observations. *J. Geophys. Res. Atmos.*, **126**, e2020JD033935, <https://doi.org/10.1029/2020JD033935>.
- Löffler-Mang, M., and J. Joss, 2000: An optical disdrometer for measuring size and velocity of hydrometeors. *J. Atmos. Oceanic Technol.*, **17**, 130–139, [https://doi.org/10.1175/1520-0426\(2000\)017<0130:AODFMS>2.0.CO;2](https://doi.org/10.1175/1520-0426(2000)017<0130:AODFMS>2.0.CO;2).
- Mellor, M., and U. Radok, 1960: Some properties of drifting snow. *Antarctic Meteorology*, Pergamon Press, 333–346.
- Newman, A. J., P. A. Kucera, and L. F. Bliven, 2009: Presenting the Snowflake Video Imager (SVI). *J. Atmos. Oceanic Technol.*, **26**, 167–179, <https://doi.org/10.1175/2008JTECHA1148.1>.
- NOAA, 2020: Winter storm severity index (WSSI)—Product description document (PDD). Accessed 2 February 2021, <https://www.wpc.ncep.noaa.gov/wwd/wssi/wssi.php>.
- Palm, S. P., Y. Yang, J. D. Spinhirne, and A. Marshak, 2011: Satellite remote sensing of blowing snow properties over Antarctica. *J. Geophys. Res.*, **116**, D16123, <https://doi.org/10.1029/2011JD015828>.
- Pettersen, C., and Coauthors, 2020: The precipitation imaging package: Assessment of microphysical and bulk characteristics of snow. *Atmosphere*, **11**, 785, <https://doi.org/10.3390/atmos11080785>.
- Rasmussen, R., and Coauthors, 2012: How well are we measuring snow: The NOAA/FAA/NCAR winter precipitation test bed. *Bull. Amer. Meteor. Soc.*, **93**, 811–829, <https://doi.org/10.1175/BAMS-D-11-00052.1>.
- Sato, T., T. Kimura, T. Ishimaru, and T. Maruyama, 1993: Field test of a new snow-particle counter (SPC) system. *Ann. Glaciol.*, **18**, 149–154, <https://doi.org/10.3189/S0260305500011411>.
- Schmidt, R. A., 1977: A system that measures blowing snow. USDA Forest Service Research Paper RM-194, 80 pp.
- Schönhuber, M., G. Lammer, and W. L. Randeu, 2007: One decade of imaging precipitation measurement by 2D-video-disdrometer. *Adv. Geosci.*, **10**, 85–90, <https://doi.org/10.5194/adgeo-10-85-2007>.
- Shimizu, H., 1963: 'Long prism' crystals observed in precipitation in Antarctica. *J. Meteor. Soc. Japan*, **41**, 305–307, https://doi.org/10.2151/jmsj1923.41.5_305.
- Stewart, R. E., and Coauthors, 1995: Winter storms over Canada. *Atmos.–Ocean*, **33**, 223–247, <https://doi.org/10.1080/07055900.1995.9649533>.
- Therrell, M. D., and M. J. Trotter, 2011: Waniyetu Wówapi: Native American records of weather and climate. *Bull. Amer. Meteor. Soc.*, **92**, 583–592, <https://doi.org/10.1175/2011BAMS3146.1>.
- Tokay, A., W. A. Petersen, P. Gatlin, and M. Wingo, 2013: Comparison of raindrop size distribution measurements by collocated disdrometers. *J. Atmos. Oceanic Technol.*, **30**, 1672–1690, <https://doi.org/10.1175/JTECH-D-12-00163.1>.
- UCAR, 2020: SNOWD UNDER. Accessed 18 January 2020, https://www.eol.ucar.edu/field_projects/snowd-under.
- Vali, G., D. Leon, and J. R. Snider, 2012: Ground-layer snow clouds. *Quart. J. Roy. Meteor. Soc.*, **138**, 1507–1525, <https://doi.org/10.1002/qj.1882>.
- Waugh, S. M., C. L. Ziegler, D. R. MacGorman, S. E. Fredrickson, D. W. Kennedy, and W. D. Rust, 2015: A balloonborne particle size, imaging, and velocity probe for in situ microphysical measurements. *J. Atmos. Oceanic Technol.*, **32**, 1562–1580, <https://doi.org/10.1175/JTECH-D-14-00216.1>.
- Wilder, L. I., 1940: *The Long Winter*. HarperCollins, 352 pp.